Published in final edited form as:
J Med Chem. 2013 February 28; 56(4): . doi:10.1021/jm4000177.

Structure Relaxivity Relationships of Serum Albumin Targeted MRI Probes Based on a Single Amino Acid Gd complex

Eszter Boros and **Peter Caravan**[*]
The Athinoula A. Martinos Center for Biomedical Imaging, Department of Radiology, Massachusetts General Hospital, Harvard Medical School, 149 Thirteenth Street, Suite 2301, Charlestown, MA 02129

Abstract

The Gd(III) complex of DO3A-N-α-amino-propionate, Gd(DOTAla), was used to generate a small library of putative MRI probes targeted to human serum albumin (HSA). Ten compounds were synthesized via multistep organic synthesis and the corresponding Gd complexes were investigated for their affinity to HSA, lipophilicity, and relaxivity in the absence and presence of HSA. Negative charge and moderate lipophilicity correlate with increased HSA affinity and relaxivity.

INTRODUCTION

Magnetic Resonance Imaging (MRI) has established itself as one of the main non-invasive imaging techniques in the clinic. This technique relies on the interaction of the proton nuclei of water with the applied magnetic field.[1] Contrast agents (or MR probes) can alter this interaction by modulating the longitudinal (T_1) or transverse (T_2) relaxation time of the surrounding proton nuclei.[2, 3] Contrast agents containing the strongly paramagnetic Gd(III) ion are suitable for shortening the T_1 of the proton nuclei of H_2O in their immediate vicinity; the Gd-induced change in T_1 normalized to contrast agent concentration is termed relaxivity, r_1. Commercial, small-molecule, non-targeted Gd-based probes have relaxivities in the 3.5 – 6.9 $mM^{-1}s^{-1}$ range when measured in blood plasma on clinical scanners.[4, 5] Subsequently, the low sensitivity of MRI commands high concentrations of these compounds in order to achieve visible contrast. Developments in recent years have focused on both the increase of relaxivity of the contrast agent in order to decrease the administered dose, as well as the specific targeting of these compounds to suitable in vivo targets.[6–8]

Human serum albumin (HSA) is the major protein component of blood plasma and serves as a transporter for both endogenous, hydrophobic compounds such as fatty acids and bilirubin as well as a vehicle for small lipophilic drug molecules.[9] HSA provides an excellent target for Gd-based T_1 agents for the purpose of blood pool imaging due to its high concentration in the bloodstream and variety of binding sites.[10, 11] HSA-binding Gd-complexes have been widely explored and one such compound, gadofosveset (aka MS-325 and sold as Vasovist or Ablavar) is approved for clinical use.[12] While gadofosveset provides greatly enhanced relaxivity in the presence of HSA compared to other commercial agents, its relaxivity is below the theoretical maximum at clinical field strengths such as 1.5T.[13] Furthermore, the ligand used to coordinate Gd is the acyclic polyamino-carboxylate DTPA, a ligand with limited kinetic inertness.[14] This has led to intense, further investigation of HSA-targeted MR

---

[*] Corresponding Author: caravan@nmr.mgh.harvard.edu, phone: 617-643-0193.

Supporting Information Available: Detailed experimental and characterization of intermediates, Gd complexes and list of nonstandard abbreviations. This material is available free of charge via the Internet at http://pubs.acs.org.

agents over the past two decades.[15–18] T_1 enhanced contrast arising from HSA targeting relies on two distinct effects: local probe accumulation due to HSA binding, and a multifold increase in relaxivity when the probe binds to HSA. This latter effect is due to the decrease of the rotational diffusion rate (molecular tumbling rate) of the Gd complex when it binds to the large HSA protein.[10] This slower tumbling rate of the paramagnetic Gd ion better approximates the proton Larmor frequency and results in increased relaxation. Tissue contrast will be greatest when both effects are maximized, i.e. when the probe is highly bound to HSA and when the relaxivity of the bound probe is optimized. Additionally, a comparably low relaxivity of the unbound probe is desirable, since this provides clearer delineation of target bound and unbound probe in vivo.

We have recently explored the application of a single amino acid type ligand system for Gd, termed DOTAla.[19] We have shown that DOTAla (DO3A-N-α-amino-propionate) derivatives form kinetically inert Gd(III) complexes with respect to Gd dechelation, We hypothesized, that this ligand scaffold would provide a convenient platform for the development of novel HSA targeting scaffolds. The overall charge under physiological conditions, the chirality of the α-carbon on DOTAla, and of course the type and combination of HSA-binding groups used is freely variable. This allows for the establishment a structure-relaxivity relationship for high relaxivity contrast agents based on the DOTAla scaffold, and for HSA targeting in general.

RESULTS AND DISCUSSION

Chemistry

DOTAla or Fmoc-DOTAla served as convenient intermediates for probe synthesis, placing the metal complex either at the C- or the N-terminus, if only one R group was conjugated (Gd(**1**), Gd(**2**), Gd(**4**), Gd(**9**)), or at the center of the corresponding artificial tripeptide structure. We chose R groups like iodinated phenols or ibuprofen derivatives with known affinity for HSA,[20] or to modify charge. For attachment to the C-terminus, glycine methyl ester, (*S*)-methylbenzylamine and 3,5-diiodo-tyrosine were used, while for attachment to the N-terminus (*S*)-methyl-benzylcarboxylate, 3,5-diiodo-tyrosine, ibuprofen or acet-amide capping was utilized. The synthesis of each ligand was performed using typical solution phase peptide synthesis (Supporting Information).

The HATU-mediated amide bond formation with N-methylmorpholine as the corresponding base was followed by HPLC purification and Fmoc deprotection using solid-support piperazine. For coupling of more than one R group, this sequence was repeated, with an additional purification step after the second Fmoc deprotection. Peptide coupling on the DOTAla scaffold results in formation of diastereomers, which were separated at a precursor stage in the case of ligand H_3(**6**), affording diastereomers H_3(**6a**) and H_3(**6b**). All other ligand systems were isolated as isomer mixtures. The final Fmoc deprotection step was generally followed by TFA-catalyzed deprotection of tert-butyl esters to afford the ready to chelate ligand; in the case of ligand H_3(**3**), the tert-butyl protected precursor for H_3(**2**) was acetylated using acetic anhydride. The corresponding crude intermediate was purified using preparative HPLC and subsequently the tert-butyl esters were removed using the same acid catalyzed deprotection conditions as used for all other ligand systems. Complex formation was achieved by dissolution of the ligand in H_2O (Scheme 1), which results in an acidic solution (pH < 3). 0.9 equivalents of $GdCl_3$ $6H_2O$ were added and the pH was slowly adjusted to 6.5 using an aqueous NaOH solution (0.1 M). Complex formation was monitored by LC-MS. Subsequent filtration and lyophilization afforded the complex as an off-white solid. For further studies, such as binding to HSA, relaxivity and lipophilicity estimates using a HPLC method, the solid was redissolved in HEPES buffer (50 mM) and filtered. The complex concentration in solution was determined using ICP-MS. The final set of compounds includes derivatives bearing R groups with presumed weak binding to HSA (Gd(**1**), Gd(**2**), Gd(**3**)), one strongly HSA binding R group (Gd(**4**), Gd(**5**), Gd(**9**)), or two strongly HSA binding R groups (Gd(**6a/6b**), Gd(**7**), Gd(**8**)).

Lipophilicity

We utilized a common HPLC method with an aqueous mobile phase at pH 6.8 to estimate lipophilicity of the metal complexes at close to physiological pH. We assumed that the measured retention time (R_t) would provide us with a good approximation for the corresponding logD of the metal complexes. Table 2 summarizes the retention times measured, including the clinically used compound MS-325. Comparison of retention times can also provide clues on how these compounds might distribute and clear in vivo. As the biological behavior of MS-325 is well known, one can hypothesize that compounds with shorter R_t than MS-325 might clear using a similar pathway (predominantly renal), while compounds with longer R_t might rely more on hepatic clearance.

HSA binding

In order to determine the binding of the complexes to HSA under physiologically relevant conditions, a well-established ultrafiltration assay was employed.[21] HSA, a 67 kDa protein, constitutes about 4.5% of plasma (0.67 mM), hence a 4.5 % w/v solution of HSA in HEPES (50 mM) was used for all related studies. Protein-complex binding was determined by ultrafiltration across a membrane with a MW 5000 cutoff and compared with the filtrate of a solution containing no HSA. The amounts of unbound and total Gd complex were measured directly by ICP-MS. A constant complex concentration of 0.1 mM was used. Binding, expressed as the fraction bound to HSA as a percentage, is found in Table 1. HSA has a great number of positively charged arginine and lysine residues within the drug binding pockets, which in turn will increase affinity for smaller, negatively charged compounds.[22] This is clearly showcased when comparing of Gd(**6a/b**) and Gd(**7**). The diastereoisomers Gd(**6a)** and Gd(**6b)** possesses a terminal, protonated amine and show similar and low affinity to HSA: only 37% binding on average. On the other hand, Gd(**7**), which differs from Gd(**6a/b**) only by replacement of the terminal amine with a terminal carboxylate, shows greatly enhanced binding by almost two fold (69%), compared to Gd(**6a/b**). Both diastereomers Gd(**6a**) and Gd(**6b**) show only small difference in percent binding, indicating that orientation of the metal complex alone has only little influence. Complexes with a net negative charge (Gd(**7**), Gd(**8**), Gd(**9**)) were found to have greatly increased affinity opposed to the neutral (Gd(**3**)) or cationic complexes (Gd(**1**), Gd(**2**), Gd(**4**), (Gd(**5**), Gd(**6a**), Gd(**6b**)). Acetylation of the primary amine (Gd(**3**)) also leads to only a slight, non-significant increase in affinity to HSA compared to the non-acetylated probe Gd(**2**). Combination of anionic charge and two strongly HSA binding R groups provides the highest % HSA binding (Gd(**8**)). The high % HSA binding of compound Gd(**8**) could be explained by either the occurrence of two separate binding events with either R group, or by binding of both R groups simultaneously. In general, there was a positive correlation between lipophilicity (R_t) and affinity (% bound), although there was considerable scatter, r^2=0.72 (Figure S1).

Lipophilicity must also be considered in the context of overall charge, which is also a dominant factor for predicting affinity. For instance cationic Gd(**6b**) and anionic Gd(**7**) have similar lipophilicity but the anionic Gd(**7**) has ~2-fold higher affinity for HSA.

Relaxivity

Relaxivity of all compounds synthesized was determined from the slope of $1/T_1$ versus Gd concentration in mM measured at 0.47 and 1.41T in the absence and presence of 4.5% w/v HSA in HEPES buffer, at compound concentrations of 0.05 – 0.4 mM (without HSA) and

0.025 – 0.15 mM (in presence of HSA). In the absence of HSA, relaxivity shows a strong positive correlation (r^2=0.94) with molecular weight, as expected (Figure S2), since the heavier complexes will tumble more slowly. The observed relaxivity r_1^{obs} in presence of HSA is the population-weighted average of the relaxivity due to the free (r_1^{free}) and bound (r_1^{bound}) probe, eq 1, where f_b and f_f are the mole fractions of bound and free, HSA unbound probe respectively.

$$r_1{}^{\mathrm{obs}}=f_f\times r_1{}^{\mathrm{free}}+f_b\times r_1{}^{\mathrm{bound}}\quad(1)$$

If the relaxivity of the HSA-bound probe is the same for all probes, then one would expect a linear relationship between percent of bound probe and observed relaxivity for all complexes. This would be true if HSA binding conferred similar rotational dynamics on all probes and did not alter water exchange kinetics. We did observe a good correlation of r_1^{obs} with % bound to a first approximation, but we found that much better correlations could be obtained if we grouped the compounds in terms of whether or not they had a C-terminal aryl substituent. Compounds with a C-terminal aryl substituent (Gd(**2**), Gd(**3**), Gd(**6a**), Gd(**6b**), Gd(**7**), Gd(**9**)) showed only moderate enhancement in relaxivity in presence of HSA. On the other hand, derivatives with no C-terminal aryl substituent (Gd(**1**), Gd(**4**), Gd(**5**), Gd(**8**)) provided considerably more enhancement of relaxivity in presence of HSA (higher r_1^{bound}). This is shown graphically in Figure 1 where extrapolation to 100% bound gives the estimated r_1^{bound}. It was found that for the group containing an aryl substituent on the C-terminus, the theoretical maximum relaxivity is considerably lower (37.8 $mM^{-1}s^{-1}$) than for compounds with an aliphatic C-terminus (50.6 $mM^{-1}s^{-1}$). There are several possible reasons for this difference: 1) the two groups of compounds could bind to different sites on HSA and each site would have different rotational dynamics; 2) there may be more internal motion associated with compounds the C-terminal aryl group and this, in turn, results in lower relaxivity; 3) or there could be other changes in compound hydration or water exchange kinetics upon binding. While the physical studies required to elucidate these differences are beyond the scope of this report, this work illustrates the need to optimize both affinity and relaxivity when developing targeted MR probes.

For the C-terminal aryl group, it was found that (*S*)-methyl-benzylamine constitutes a rather poor binding group, which does not lead to great increase of either binding or relaxivity. Predominant factors with influence on relaxivity are charge and choice of the HSA binding R group. The binding pockets on HSA are often described as deep, “sock-shaped” cavities with a high density of cationic charge facilitating binding of smaller, anionic molecules. This is readily showcased with compounds from the aliphatic C terminus group. Binding and observed relaxivity is highest for one of the smallest compounds of the entire compound series, Gd(**9**). The mono-anionic charge of the complex likely increases the possibility for tight binding of the complex itself through hydrogen bonding to the binding pocket, while the strongly HSA binding R group is already in place and is able bind simultaneously and further rigidify the structure of the bound probe.

MR imaging

In order to illustrate how observed relaxivity in presence of HSA compares to relaxivity in the unbound state, a T_1 weighted image was acquired for a series of 0.1 mM probe concentration in the absence of presence of 4.5% HSA (Figure 2). The clinically used contrast agent MS-325 is shown as a reference (far left), showing increased signal in presence of HSA when compared with the MS-325 solution without HSA. Gd(**8**), which has the highest affinity for HSA among the compounds investigated, provides high signal in the presence of HSA (right). However Gd(**8**) also had the highest relaxivity in the absence of

HSA and this results in the highest signal in the absence of HSA compared to MS-325 or Gd(**9**). This high relaxivity of Gd(**8**) in the unbound state results in lower contrast between the samples with and without HSA (two tubes on right). Gd(**9**) provides the greatest contrast between the free and HSA-bound states (middle two tubes) due to a considerably shorter rotational correlation time of the unbound molecule, but also a comparably high observed relaxivity in presence of HSA.

This large change in relaxivity upon binding and resultant increase in contrast for Gd(**9**) is highly advantageous for in vivo applications, making it an interesting candidate for future animal studies.

CONCLUSION

Ten derivatives of Gd(DOTAla) (DO3A-N-α-amino-propionate) were synthesized with different relaxivities and affinities for human serum albumin. We found that changes in affinity are dominated by complex charge and choice of binding groups. A combination of anionic charge and two strong binding groups provides greatest affinity (Gd(**8**)). However, while the combination of strong HSA binding substituents might increase the fraction bound to HSA, it does not necessarily result in the highest observed relaxivity. We found that the small, monoanionic complex Gd(**9**) showed the highest relaxivity in the presence of HSA, possibly due to a more efficient decrease of rotational freedom. Gd(**9**) also provides the greatest increase in relaxivity in presence of HSA when compared to the unbound probe. It compares well to values found for MS-325. The ease of functionalization of the DOTAla scaffold does not limit applications of this moiety to HSA, but ultimately provides an optimal platform for exploration of targeted, high relaxivity Gd-based T_1 agents.

EXPERIMENTAL SECTION

Chemistry

^1H and ^{13}C NMR spectra were recorded on a Varian 11.7 T NMR system. The purity of tested compounds as determined by analytical HPLC with absorbance at 220 nm was >95%. Estimation of lipophilicity of complexes Gd(**1**) through Gd(**9**) as well as MS-325 was also carried out using method C: Mobile phases: A (ammonium formate, 20 mM, pH 6.8); B (9:1 MeCN/20 mM ammonium formate), flow-rate 0.8 mL/min, Gradient: 0 – 40 min: 0 – 95 % B, 40 – 43 min: 95% B, 43 – 43.5 min: 95 - 0 % B, 43.5 – 45 min: 0 % B. Further experimental details and characterization of intermediates using ^1H and ^{13}C NMR, as well as ESI-LCMS are outlined in the supporting information, together with ESI-MS data and synthetic procedure for Gd-complexes. The ligands H_3(**1**) – H_4(**9**) were afforded using general procedure 3 (supporting information). The solvent is removed *in vacuo* and the product is isolated as the trifluoroacetate salt. For the formation of Gd complexes Gd(**1**) – Gd(**9**), general procedure 4 was used (supporting information).

2,2′,2″-(10-(2-amino-3-((2-methoxy-2-oxoethyl)amino)-3-oxopropyl)-1,4,7,10-tetraazacyclododecane-1,4,7-triyl)tri-acetic acid, H_3(1)—^1H-NMR (D_2O, 500 MHz, ppm): 3.64 -3.63 (m, 5H), 3.51 (s, 3H), 3.51 – 2.58 (m, 22H). ^{13}C-NMR (D_2O, 125 MHz, ppm): 175.8, 171.6, 170.4, 170.3, 58.1, 56.7, 53.9, 52.9, 52.4, 50.4, 48.9, 46.0, 41.22. LC-ESI-MS: calcd. for $C_{20}H_{37}N_6O_9$: 505.25 Found: 505.3 $[M+H]^+$.

2,2′,2″-(10-(2-amino-3-oxo-3-(((S)-1-phenylethyl)amino) propyl)-1,4,7,10-tetraazacyclododecane-1,4,7-triyl)triacetic acid, H_3(2)—^1H-NMR (D_2O, 500 MHz, ppm): 7.45 – 7.37 (m, 5H), 4.98 – 4.96 (m, 1H), 3.51 (m, 1H), 3.19 - 2.26 (m, 23H), 1.51 (t, 3H). ^{13}C-NMR (D_2O, 125 MHz, ppm): 179.0, 176.6, 128.8, 128.7, 126.0, 125.8, 59.3, 49.4, 21.1. LC-ESI-MS: calcd. for $C_{25}H_{41}N_6O_7$: 537.3 Found: 537.3 $[M+H]^+$.

2,2′,2″-(10-(2-acetamido-3-oxo-3-(((S)-1-phenylethyl)amino) propyl)-1,4,7,10-tetraazacyclododecane-1,4,7-triyl)triacetic acid H_3(3)—^{1}H-NMR (CD_3OD, 500 MHz, ppm): 8.4 (s, 1H) 7.29 - 7.15 (m, 5H), 4.95 (s, 1H), 4.01 – 2.85 (m, 24H), 1.91 (s, 3H), 1.39 (t, 3H). ^{1}H-NMR (CD_3OD, 125 MHz, ppm): 178.3, 154.4, 147.3, 143.2, 128.2, 126.8, 125.9, 56.0, 55.7, 53.3, 50.6, 49.1, 48.4, 29.3, 15.6. LC-ESI-MS: calcd. for $C_{27}H_{43}N_6O_8$: 579.3 Found: 579.3 $[M+H]^+$.

2,2′,2″-(10-(2-(2-amino-3-(4-hydroxy-3,5-diiodophenyl) propanamido)-2-carboxyethyl)-1,4,7,10-tetraazacyclododecane-1,4,7-triyl)triacetic acid, H_4(4)—^{1}H-NMR (D_2O, 500 MHz, ppm): 7.8 – 7.66 (d, 2H), 4.33 (d, 1H), 4.34 (d, 1H), 3.89 – 2.54 (m, 24H). ^{13}C-NMR (D_2O, 125 MHz, ppm): 174.9, 169.5, 154.3, 140.9, 131.1, 124.7, 84.8, 54.4, 51.9, 47.9, 35.2, 28.3. LC-ESI-MS: calcd. for $C_{26}H_{39}I_2N_6O_{10}$: 849.1. Found: 849.1 $[M+H]^+$.

2,2′,2″-(10-(2-(2-amino-3-(4-hydroxy-3,5-diiodophenyl) propanamido)-3-((2-methoxy-2-oxoethyl) amino)-3-oxopropyl)-1,4,7,10- tetraazacyclododecane-1,4,7-triyl)triacetic acid, H_3(5)—^{1}H-NMR (D_2O, 500 MHz, ppm): 7.69 (s, 2H), 4.62 (d, 1H), 4.18 (s, 1H), 3.94 -2.80 (m, 30H). ^{13}C-NMR (D_2O, 125 MHz, ppm): 171.0, 170.6, 170.1, 160.8, 160.5, 154.9, 140.8, 140.3, 129.4, 117.5, 115.1, 84.4, 84.0, 61.9, 56.1, 53.8, 53.1, 51.5, 51.3, 40.9. LC-ESI-MS: calcd. for $C_{29}H_{44}I_2N_7O_{11}$: 920.1 Found: 920.1 $[M+H]^+$.

2,2′,2″-(10-(2-(2-amino-3-(4-hydroxy-3,5-diiodophenyl) propanamido)-3-oxo-3-(((S)-1-phenylethyl)amino)propyl)-1,4,7,10-tetraazacy clodo-decane-1,4,7-triyl)triacetic acid, H_3(6a/b)—^{1}H-NMR (CD_3OD, 500 MHz, ppm): 8.38 (d, 1H) 7.65 (d, 2H), 7.33 – 7.24 (m, 5H), 4.98 (d, 1H), 4.76 – 4.03 (m, 5H), 3.64 – 2.50 (m, 18H), 1.51 – 1.39 (t, 3H). ^{13}C-NMR (CD_3OD, 125 MHz, ppm): 169.7, 169.2, 160.2, 159.9, 154.9, 142.9, 140.6, 129.7, 128.1, 126.8, 125.9, 117.4, 114.8, 89.4, 81.2, 81.1, 53.8, 53.3, 51.3, 50.9, 49.0, 48.2, 34.3. LC-ESI-MS: calcd. for $C_{34}H_{48}I_2N_7O_9$: 952.2 Found: 952.2 $[M+H]^+$.

2,2′,2″-(10-(3-(((S)-1-carboxy-2-(4-hydroxy-3,5-diiodophenyl) ethyl) amino)-3-oxo-2-((S)-2-phenylpropan-amido)propyl)-1,4,7,10-tetraaza-cyclododecane-1,4,7-triyl) triacetic acid, H_3(7)—^{1}H-NMR (CD_3OD, 500 MHz, ppm): 7.97 (d, 1H), 7.61 – 7.28 (m, 7H), 4.66 (m, 1H), 4.02 - 2.61 (m, 26H), 1.59 (m, 3H). ^{13}C-NMR (CD_3OD, 125 MHz, ppm): 171.0, 168.2, 161.2, 156.8, 142.4, 141.1, 139.9, 127.1, 126.8, 122.2, 121.3, 117.4, 83.9, 65.1, 49.2, 31.2. LC-ESI-MS: calcd. for $C_{35}H_{47}I_2N_6O_{11}$: 981.1. Found: 981.1 $[M+H]^+$.

2,2′,2″-(10-(3-((1-carboxy-2-(4-hydroxy-3,5-diiodophenyl) ethyl)amino) -2-(2-(4-isobutylphenyl)propan-amido)-3-oxopropyl)-1,4,7,10-tetraaza-cyclododecane-1,4,7-triyl)triacetic acid, H_3(8)—^{1}H-NMR (D_2O, 500 MHz, ppm): 7.52 (d, 2H), 7.16 – 7.00 (m, 4H), 4.48 (m, 1H), 3.86 - 2.85 (m, 22H), 1.78 (m, 2H), 1.78 (m, 1H), 1.21 (m, 3H) 0.81 (m, 6H). ^{13}C-NMR (D_2O, 125 MHz, ppm): 171.0, 170.6, 161.2, 153.2, 142.1, 140.6, 139.9, 129.3, 128.8, 128.1, 126.8, 83.9, 65.1, 53.4, 34.6, 30.0, 29.4, 27.4, 24.7, 22.3, 21.5, 21.3. LC-ESI-MS calcd. for $C_{39}H_{55}I_2N_6O_{11}$: 1037.2. Found: 1037.1 $[M+H]^+$.

2,2′,2″-(10-(2-carboxy-2-(2-(4-isobutylphenyl) propanamido) ethyl)-1,4,7,10-tetraazacyclododecane-1,4,7-triyl)triacetic acid, H_4(9)—^{1}H-NMR (D_2O, 500 MHz, ppm): 7.26 (d, 2H), 7.20 (d, 2H), 3.73 -2.83 (m, 26H), 2.43 (m, 2H), 1.78 (t, 1H), 1.41 (d, 3H), 0.81 (m, 6H). ^{13}C-NMR (D_2O, 125 MHz, ppm):. ^{13}C-NMR (D_2O, 125 MHz, ppm):

177.5, 176.9, 141.9, 138.5, 130.1, 127.3, 70.2, 54.4, 46.5, 44.8, 30.7, 27.8, 22.8. LC-ESI-MS: calcd. for $C_{30}H_{48}N_5O_9$: 622.3 Found: 622.4 $[M+H]^+$.

Supplementary Material

Refer to Web version on PubMed Central for supplementary material.

Acknowledgments

Funding Sources

This work was supported in part by awards R01EB009062 from the National Institute of Biomedical Imaging and Bioengineering (NIBIB) and P41RR14075 from the National Center for Research Resources (NCRR).

E.B. acknowledges the Swiss National Science Foundation for a fellowship for prospective researchers. Nathaniel Kenton is acknowledged for synthesis of DOTAla and Fmoc-DOTAla according to reference.[19]

References

1. Young, IR. Methods in Biomedical Magnetic Resonance Imaging and Spectroscopy. John Wiley & Sons Ltd; Chichester: 2000.
2. Caravan P, Ellison JJ, McMurry TJ, Lauffer RB. Gadolinium(III) Chelates as MRI Contrast Agents: Structure, Dynamics, and Applications. Chem Rev. 1999; 99:2293–2352. [PubMed: 11749483]
3. Manus LM, Strauch RC, Hung AH, Eckermann AL, Meade TJ. Analytical Methods for Characterizing Magnetic Resonance Probes. Anal Chem. 2012; 84:6278–6287. [PubMed: 22624599]
4. Caravan P. Strategies for Increasing the Sensitivity of Gadolinium based MRI Contrast Agents. Chem Soc Rev. 2006; 35:512–523. [PubMed: 16729145]
5. Rohrer M, Bauer H, Mintorovitch J, Requardt M, Weinmann H. Comparison of Magnetic Properties of MRI Contrast Media Solutions at Different Magnetic Field Strengths. Invest Radiol. 2005; 40:715–724. [PubMed: 16230904]
6. Caravan P, Zhang Z. Structure–Relaxivity Relationships among Targeted MR Contrast Agents. Eur J Inorg Chem. 2012:1916–1923. [PubMed: 22745568]
7. Terreno E, Dastru W, Castelli DD, Gianolio E, Crich SG, Longo D, Aime S. Advances in Metal-based Probes for MR Molecular Imaging Applications. Curr Med Chem. 2010; 17:3684–3700. [PubMed: 20846110]
8. Chan KWY, Wong WT. Small Molecular Gadolinium(III) Complexes as MRI Contrast Agents for Diagnostic Imaging. Coord Chem Rev. 2007; 251:2428–2451.
9. Carter DC, Ho JX. Structure of Serum Albumin. Adv Protein Chem. 1994; 45:153–203. [PubMed: 8154369]
10. Caravan P. Protein-Targeted Gadolinium-Based Magnetic Resonance Imaging (MRI) Contrast Agents: Design and Mechanism of Action. Acc Chem Res. 2009; 42:851–862. [PubMed: 19222207]
11. Aime S, Botta M, Fasano M, Crich SG, Terreno E. Gd(III) Complexes as Contrast Agents for Magnetic Resonance Imaging: A Proton Relaxation Enhancement Study of the Interaction with Human Serum Albumin. J Biol Inorg Chem. 1996; 1:312–319.
12. Caravan P, Cloutier NJ, Greenfield MT, McDermid SA, Dunham SU, Bulte JWM, Amedio JC, Looby RJ, Supkowski RM, Horrocks WD, McMurry TJ, Lauffer RB. The Interaction of MS-325 with Human Serum Albumin and its Effect on Proton Relaxation Rates. J Am Chem Soc. 2002; 124:3152–3162. [PubMed: 11902904]
13. Caravan P, Farrar CT, Frullano L, Uppal R. Influence of Molecular Parameters and Increasing Magnetic Field Strength on Relaxivity of Gadolinium- and Manganese-based T1 Contrast Agents. Contrast Media Mol Imaging. 2009; 4:89–100. [PubMed: 19177472]

14. Laurent S, Vander Elst L, Copoix F, Muller RN. Stability of MRI Paramagnetic Contrast Media: A Proton Relaxometric Protocol for Transmetallation Assessment. Invest Radiol. 2001; 36:115–122. [PubMed: 11224760]
15. Ou MH, Tu CH, Tsai SC, Lee WT, Liu GC, Wang YM. Synthesis and Physicochemical Characterization of Two Gadolinium(III) TTDA-like Complexes and Their Interaction with Human Serum Albumin. Inorg Chem. 2006; 45:244–254. [PubMed: 16390062]
16. Henoumont C, Elst LV, Laurent S, Muller RN. Synthesis and Physicochemical Characterization of Gd-C4-Thyroxin-DTPA, a Potential MRI Contrast Agent. Evaluation of Its Affinity for Human Serum Albumin by Proton Relaxometry, NMR Diffusometry, and Electrospray Mass Spectrometry. J Phys Chem. 2010; 114:3689–3697.
17. Chang YH, Chen CY, Singh G, Chen HY, Liu GC, Goan YG, Aime S, Wang YM. Synthesis and Physicochemical Characterization of Carbon Backbone Modified $[Gd(TTDA)(H_2O)]^{2-}$ Derivatives. Inorg Chem. 2011; 50:1275–1287. [PubMed: 21247114]
18. Nivorozhkin AL, Kolodziej AF, Caravan P, Greenfield MT, Lauffer RB, McMurry TJ. Enzyme-Activated Gd3+ Magnetic Resonance Imaging Contrast Agents with a Prominent Receptor-Induced Magnetization Enhancement. Angew Chem Int Ed. 2001; 40:2903–2906.
19. Boros E, Polasek M, Zhang Z, Caravan P. Gd(DOTAla) – A Single Amino Acid Gd-complex as a Modular Tool for High Relaxivity MR Contrast Agent Development. J Am Chem Soc. 2012; 134:19858–19868. [PubMed: 23157602]
20. Peters, T. All about Albumin. Academic Press; San Diego: 1996.
21. McMurry TJ, Parmelee DJ, Sajiki HS, DM, Ouellet HS, Walovitch RC, Tyeklar Z, Dumas S, Bernard P, Nadler S, Midelfort K, Greenfield M, Troughton J, Lauffer RB. The Effect of a Phosphodiester Linking Group on Albumin Binding Blood half-life Relaxivity of Intravascular Diethylenetriaminepentaacetato Aquo Gadolinium(III) MRI Contrast Agents. J Med Chem. 2002; 45:3465–3474. [PubMed: 12139457]
22. Aime S, Gianolio E, Longo D, Pagliarin R, Lovazzano C, Sisti M. New Insights for Pursuing High Relaxivity MRI Agents from Modelling the Binding Interaction of GdIII Chelates to HSA. ChemBioChem. 2005; 6:818–820. [PubMed: 15791689]
23. Caravan P, Parigi G, Chasse JM, Cloutier NJ, Ellison JJ, Lauffer RB, Luchinat C, McDermid SA, Spiller M, McMurry TJ. Albumin Binding, Relaxivity, and Water Exchange Kinetics of the Diastereoisomers of MS-325, a Gadolinium(III)-Based Magnetic Resonance Angiography Contrast Agent. Inorg Chem. 2007; 46:6632–6639. [PubMed: 17625839]

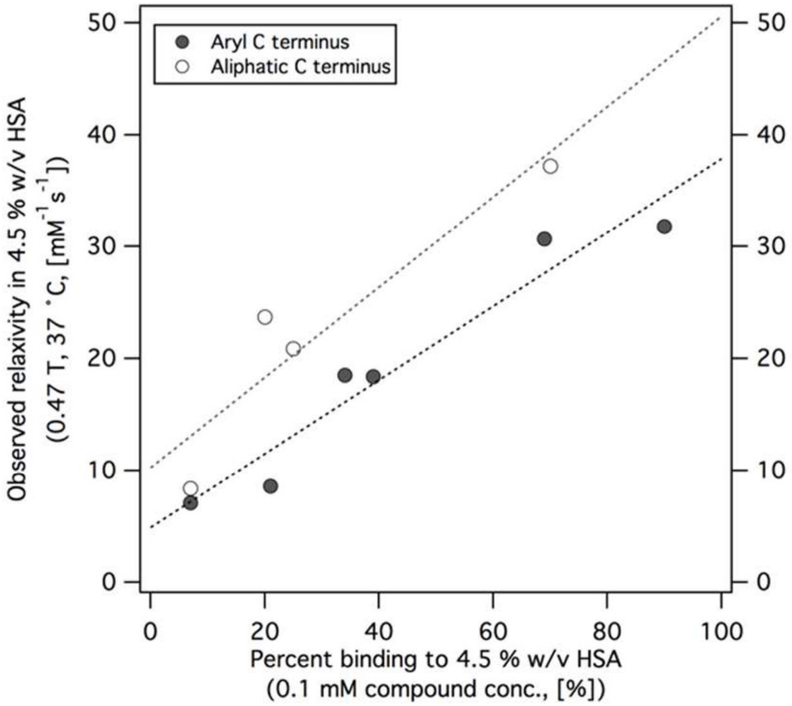

Figure 1.

Correlation plots of observed relaxivity in HSA versus percent binding to HSA. Compounds were split in two categories: C-terminal aryl substituent (filled symbols) (Gd(**2**), Gd(**3**), Gd(**6a**), Gd(**6b**), Gd(**7**), Gd(**9**)) and C-terminal aliphatic substituent (open symbols) (Gd(**1**), Gd(**4**), Gd(**5**), Gd(**8**)).

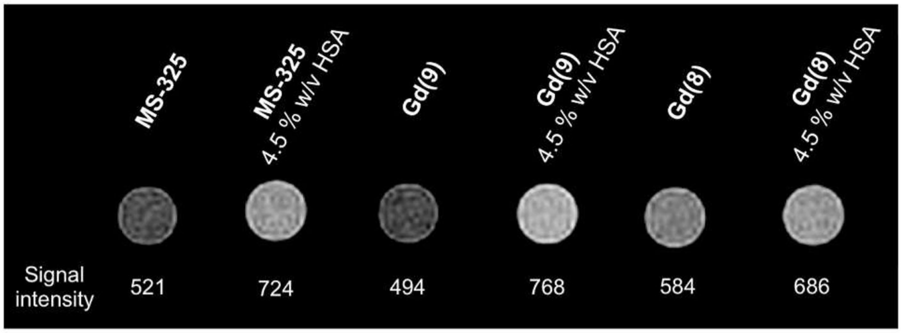

Figure 2.

T_1 weighted image of compounds MS-325, Gd(**8**) and Gd(**9**) with measured signal intensity listed beneath each sample. Samples contain 0.1 mM compound, with or without 4.5 % w/v HSA. TR/TE/flip angle = 25ms/ 4.7ms/ 70°.

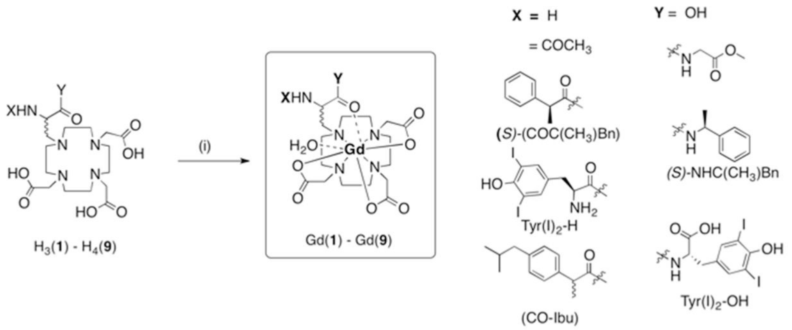

Scheme 1.

General structure and synthetic scheme for derivatives H_3(**1**) through H_4(**9**) as well as the corresponding Gd complexes Gd(**1**) through Gd(**9**). (i) $GdCl_3$ $6H_2O$, H_2O/MeOH (1:1), pH 6.5.

Table 1

Numbering scheme of compounds synthesized and investigated for this study.

Compound	-X	-Y
Gd(**1**)	H	Gly-OMe
Gd(**2**)	H	(*S*)-NHC(CH_3)Bn
Gd(**3**)	$COCH_3$	(*S*)-NHC(CH_3)Bn
Gd(**4**)	Tyr(I)$_2$-H	OH
Gd(**5**)	Tyr(I)$_2$-H	Gly-OMe
Gd(**6a**)	Tyr(I)$_2$-H	(*S*)-NHC(CH_3)Bn
Gd(**6b**)	Tyr(I)$_2$-H	(*S*)-NHC(CH_3)Bn
Gd(**7**)	(*S*)-COC(CH_3)Bn	Tyr(I)$_2$-OH
Gd(**8**)	CO-Ibu	Tyr(I)$_2$-OH
Gd(**9**)	CO-Ibu	H

Table 2

Summary of lipophilicity (as retention times), relaxivity (r_1) in 50 mM HEPES buffer (pH 7.4, 37 °C) in the absence (r_1^{free}) or presence (r_1^{obs}) of 4.5% HSA at 0.47 and 1.41 T, and percent of 0.1 mM probe concentration bound to 4.5% w/v HSA. The error in the binding and relaxivity data is estimated to be ±10% of the measured value.

		0.47T		1.41T		
	Lipophilicity (Rt)	**r_1^{free} ($mM^{-1}s^{-1}$)**	**r_1^{obs} ($mM^{-1}s^{-1}$) 4.5% HSA**	**r_1^{free} ($mM^{-1}s^{-1}$)**	**r_1^{obs} ($mM^{-1}s^{-1}$) 4.5% HSA**	**% bound to 4.5% HSA**
Gd(1)	7.0	4.5	8.4	4.1	7.6	7%
Gd(2)	6.0	4.8	7.1	3.9	5.9	7%
Gd(3)	12.4	5.2	8.6	4.5	6.3	21%
Gd(4)	8.9	6.1	23.7	5.8	17.4	20%
Gd(5)	11.0	6.9	20.9	6.3	16.7	25%
Gd(6a)	12.7	7.1	18.5	6.6	10.9	34%
Gd(6b)	14.1	6.8	18.4	6.1	11.7	39%
Gd(7)	12.3	6.5	30.7	6.0	21.8	69%
Gd(8)	17	7.1	31.8	6.7	21.1	90%
Gd(9)	14.7	5.6	37.2	4.8	22.4	70%
MS-325	11.2	6.6[a]	42 [a]	5.5 [a]	23.8 [a]	88% [a]

[a] from Reference.[23]